

Interactions in the PSR J0737–3039 System

R. N. Manchester,¹ A. G. Lyne,² M. Burgay,³ M. Kramer,² A. Possenti,^{4,5} F. Camilo,⁶ A. W. Hotan,⁷ M. A. McLaughlin,² D. R. Lorimer,² N. D’Amico,^{5,8} B. C. Joshi,⁹ J. E. Reynolds,¹ P. C. C. Freire¹⁰.

¹*Australia Telescope National Facility, CSIRO, Australia,* ²*University of Manchester, Jodrell Bank Observatory, UK,* ³*Universita degli Studi di Bologna, Italy,* ⁴*INAF-Osservatorio Astronomica di Bologna, Italy,* ⁵*INAF-Osservatorio Astronomica di Cagliari, Italy,* ⁶*Columbia University, USA,* ⁷*Swinburne University of Technology, Australia,* ⁸*Universita degli Studi di Cagliari, Italy,* ⁹*NCRA, Puna, India,* ¹⁰*NAIC, Arecibo Observatory, Puerto Rico.*

Abstract. The double-pulsar system PSR J0737–3039 offers a unique opportunity to probe the magnetospheric processes in pulsars. The pulse emission from PSR J0737–3039B, the younger and slower of the two pulsars, is strongly modulated as a function of orbital phase. Short eclipses of the A pulsar emission are also observed. Progress on understanding these phenomena poses substantial observational and theoretical challenges.

1. Introduction

The discovery of the relativistic binary pulsar PSR J0737–3039 was announced by Burgay et al. (2003) and is summarised by Burgay et al., in this volume. This pulsar has a 22-ms period and is in a 2.4-hr orbit with a neutron-star companion. The detection of this companion as a 2.8-s pulsar, announced by Lyne et al. (2004), makes this the first known double-pulsar binary system. Even before the discovery of pulsed emission from the companion, PSR J0737–3039A (as the 22-ms pulsar is now known) held promise of being a superb probe of theories of relativistic gravity. This promise has been greatly enhanced by the detection of PSR J0737–3039B as described by Lyne et al. (2004) and further discussed by Kramer et al., in this volume. The double pulsar is not only a superb test-bed for relativistic gravity—it also provides an unprecedented opportunity to probe the workings of pulsar magnetospheres. The pulse emission from the B pulsar is strongly modulated with orbital phase, most probably as a consequence of the penetration of the A-pulsar wind into B’s magnetosphere. Furthermore, eclipses of the A pulse emission by B’s magnetosphere are observed.

These phenomena and some of their implications are discussed in this paper. To assist with this discussion, relevant parameters for the two pulsars are given in Table 1.

Table 1. Parameters for PSRs J0737–3039A and B

	PSR J0737–3039A	PSR J0737–3039B
Pulse Period	22.7 ms	2.77 s
Period derivative	1.7×10^{-18}	0.88×10^{-15}
Surface dipole magnetic field	6.4×10^9 G	1.6×10^{12} G
Light-cylinder radius	1080 km	1.32×10^5 km
Magnetic field at light cylinder	5.1×10^3 G	0.70 G
Spin-down luminosity	5.9×10^{33} erg s ⁻¹	1.6×10^{30} erg s ⁻¹
Orbit semi-major axis	424,000 km	453,000 km
Mean orbit velocity	301 km s ⁻¹	323 km s ⁻¹

2. Orbital Modulation of PSR J0737–3039B

PSR J0737–3039B was not detected in the original discovery observation. It is now clear that this is because pulses from the B pulsar are only strong for two short intervals each orbit. The discovery observation happened to be at a time when B was not pulsing. Figure 1 shows the B pulse intensity as a function of pulse phase and orbital longitude for two frequency bands centered at 680 and 3100 MHz respectively.¹ The first burst of strong emission, centered near orbital longitude 210°, covers about 40° of longitude (~ 13 min) and the second, centered near longitude 280°, covers about 25° of longitude (~ 8 min). Each of these plots represents a sum over several orbits; there is no discernible variation of the modulation pattern from orbit to orbit.

Figure 1 shows that not only does the pulse intensity change with orbital phase, the pulse shape changes as well! At the start of the first burst the pulse has a strong trailing component and a weaker leading component which dies out in the later phases of the burst. The component separation is about 5° of pulse longitude (37 ms). In the second burst, there are two components of similar amplitude, initially separated by about 5.5° (42 ms). The trailing component moves steadily to later phases during the burst, increasing the component separation to about 6.5° (50 ms) at the end.

The orbital modulation of the pulse intensity is broadly independent of frequency, at least over the observed range (Fig. 1). However, the components are broader at the lower frequency and are well represented by a convolution of the high-frequency profiles with a smoothing function of width about 2°.

Although the B pulsar is only strong for these two short intervals, pulsed emission is weakly present at most other orbital phases. At longitudes 0 – 30° (Fig. 1), it has an amplitude about 10 percent of that in the first burst, whereas at other longitudes it is $\lesssim 3$ percent.

Using the parameters from Table 1, the energy density at the B pulsar of the wind resulting from spin-down of the A pulsar is about 2.1 erg cm⁻³. This is about two orders of magnitude greater than the energy density (or equivalently, pressure)

¹These and other plots in this paper were produced using the PSRCHIVE pulsar data analysis package (Hotan, van Straten, & Manchester 2004).

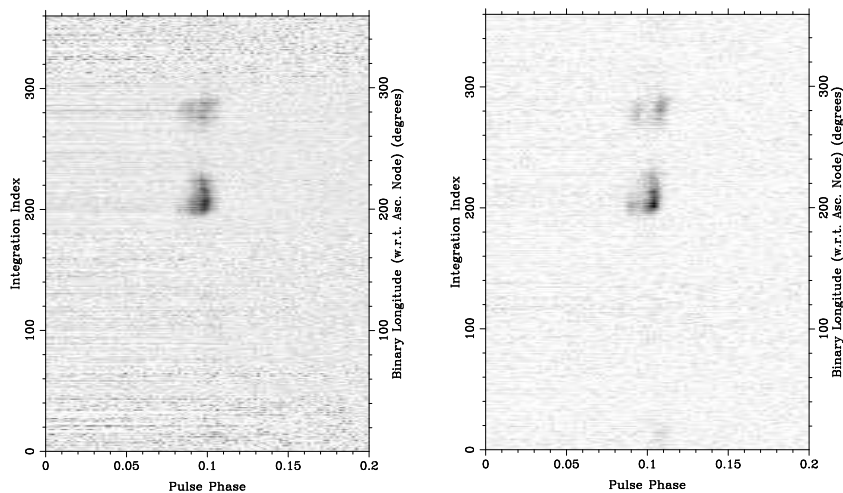


Figure 1. Intensity of PSR J0737–3039B as a function of pulse phase and orbital longitude (with respect to the ascending node) for two wavelength bands, 50cm (680 MHz) and 10cm (3100 MHz). The entire orbital period but only 20 percent of the pulse period is shown for each plot. Inferior conjunction, when the the two pulsars are most closely aligned with the B pulsar on the near side, is at orbital longitude 270°. Each of the two plots represents the sum of about 15.5 hours of data.

of the B pulsar wind at its light cylinder. Hence, the A wind will penetrate deep into the B-pulsar magnetosphere. The penetration depth is determined by pressure balance between the A wind and the B dipolar magnetic field giving an effective Alfvén radius of about $0.45 R_{LC}$. This implies that 90 percent of the B-pulsar magnetosphere is blown away by the A wind!

There can be little doubt that the observed orbital modulations of the B pulse shape and intensity are due to interactions of the A wind with the emission process. The fact that B is able to function as a pulsar at all implies that the emission region lies within the Alfvén radius and therefore is not located near the light cylinder. The degree of penetration of the A wind into B’s magnetosphere will be a function of B’s spin phase and, provided there is some misalignment between B’s spin axis and the orbital angular momentum vector, orbital phase and spin precessional phase. We expect changes in the modulation pattern as the spin axes of the two pulsars precess. The two strong bursts occur when B is close to inferior conjunction. If the beamed emission is associated with open field lines from a polar-cap region, then the bursts occur when the lines are open approximately in the A-wind direction. However, this simple fact alone does not account for the complex observed modulation.

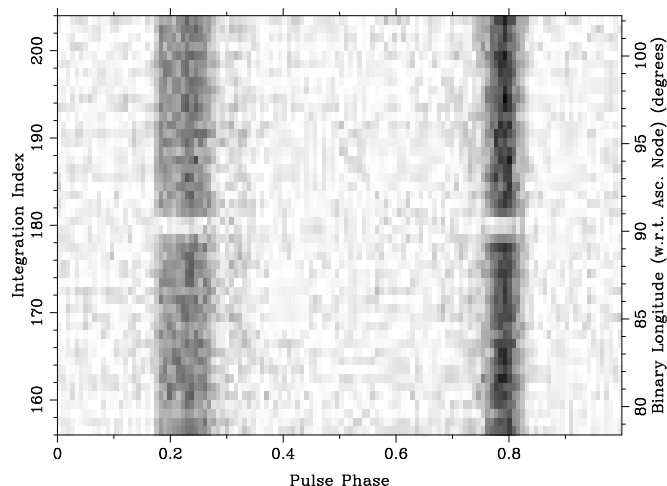


Figure 2. Intensity of PSR J0737–3039A as a function of pulse phase and orbital longitude (with respect to the ascending node) at 20 cm wavelength (1390 MHz). Approximately 20.2 hours of data with a sub-integration time of 10 s were summed to form this plot.

3. The Eclipse of PSR J0737–3039A

Figure 2 illustrates the eclipse of the A pulsar at superior conjunction (90° orbital longitude). The eclipse is very short with a duration of less than 30 s centered slightly after conjunction. Observations at the 50 cm and 10 cm bands show that within the uncertainties the eclipse duration is independent of frequency. Given that the relative orbital velocity of the two stars is about 620 km s^{-1} , a 30-s eclipse corresponds to a width of the eclipsing region at the B pulsar of about 18,000 km or about $0.14 R_{LC}$ (Table 1). Observations of relativistic timing perturbations show that the orbit inclination is $87^\circ.7^{+1^\circ.7}_{-2^\circ.9}$ (Kramer et al., in this volume). The best estimate ($87^\circ.7$) corresponds to an impact parameter of about 35,400 km or $0.26 R_{LC}$ at the B pulsar, much greater than the width of the eclipsing region. This suggests that the eclipse results from a grazing impact on an eclipsing region of radius about $0.27 R_{LC}$. Alternatively, the orbit inclination may be even closer to 90° , in which case the eclipsing region has a radius of between $0.07 R_{LC}$ and $0.27 R_{LC}$.

4. Mean Pulse Polarization

As well as giving information on the pulse emission mechanism(s), polarization observations potentially provide an important probe into the plasma conditions within the orbit and, in particular, within B’s magnetosphere. Figure 3 shows mean pulse polarization profiles for A (averaged over one orbit) at 20 cm and for B (averaged over a leading burst) at 50 cm. The time-reversal symmetry of A’s pulse shape and linear polarization about phase 0.5 (as plotted) and the flat

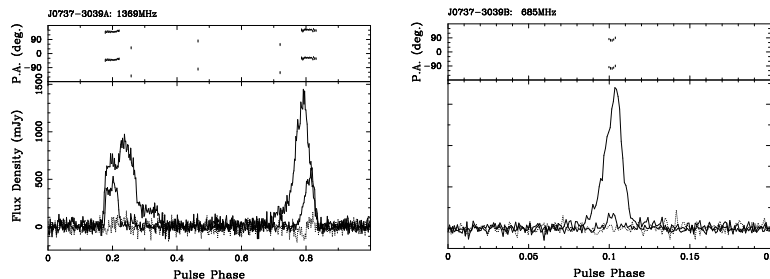


Figure 3. Mean pulse polarization profiles for PSR J0737–3039A at 20 cm (left) and PSR J0737–3039B at 50 cm (right) obtained with the ATNF wide-band correlator. In each plot, the darker solid line is the total intensity (Stokes I), the fainter solid line is the linearly polarized intensity and the dotted line is circularly polarized intensity (Stokes V). The position angle (with arbitrary zero) of the linearly polarized component is shown in the upper part. Data at both frequencies have been corrected for an interstellar Faraday rotation of -120 rad m^{-2} . Note the expanded scale on the right plot.

position-angle variations are all consistent with the A pulsed emission originating from field lines associated with a single magnetic pole in a very wide emission beam, similar to that proposed for PSR B1259–63 (Manchester & Johnston 1995). The B pulse profile is about 10 percent linearly polarized near the pulse peak and has no significant circular polarization. The linear polarization observed in both pulsars will facilitate investigations of plasma conditions within the system.

5. Unpulsed Emission

There is some evidence for significant unpulsed emission from the system. The mean pulsed flux density of A at 20 cm is about 1.6 mJy (Lyne et al. 2004). During the first burst, B’s 20-cm flux density is similar, but its duty cycle is only about 15 percent so it makes a small contribution to the long-term mean. In contrast, a 6-hour synthesis image using the Australia Telescope Compact Array (Burgay et al. 2003) gave a mean flux density of $\sim 6 \text{ mJy}$ at 20 cm. While this result needs confirmation, taken at face value it implies substantial unpulsed emission from the system. The spectrum and origin of this unpulsed emission are presently unknown.

6. Challenges for the Future

The double-pulsar system presents some wonderful opportunities for interesting and important science in a number of areas. Achieving these goals poses a

number of challenges – for both observational and theoretical astronomers. Some of the more significant questions and challenges are listed here.

- Separation of B's intrinsic pulse-shape changes from orbit-phase-dependent timing perturbations
- Separation of spin-precession effects from secular changes in pulse period and orbital parameters
- Obtaining high time-resolution multi-frequency polarization observations across the A eclipse
- Understanding of the interaction between the A wind and the B magnetosphere
- Are magnetic field strengths computed from the usual dipole relation valid for B?
- Does the B pulsed emission originate from a magnetic polar region and why is it modulated as a function of orbital phase?
- What is the mechanism for the eclipses of A?
- Where does the unpulsed emission from the system originate?
- Is the almost edge-on aspect of the orbit just good fortune?

It is clear that understanding this system will keep many of us busy for a long time!

Acknowledgments. The Parkes radio telescope is part of the Australia Telescope which is funded by the Commonwealth of Australia for operation as a National Facility managed by CSIRO.

References

- Burgay, M., et al. 2003, *Nature*, 426, 531
Hotan, A., van Straten, W., & Manchester, R. N. 2004, *PASA*, 21, 302
Lyne, A. G., et al. 2004, *Science*, 303, 1153
Manchester, R. N., & Johnston, S. 1995, *ApJ*, 441, L65